Suppression of antiphase domain boundary formation in $Ba_{0.5}Sr_{0.5}TiO_3$ films grown on vicinal MgO substrates

Cite as: Appl. Phys. Lett. **85**, 2905 (2004); https://doi.org/10.1063/1.1804609
Submitted: 13 May 2004 . Accepted: 11 August 2004 . Published Online: 14 October 2004

H. Zheng, L. Salamanca-Riba, R. Ramesh, and H. Li

Suppression of antiphase domain boundary formation in $Ba_{0.5}Sr_{0.5}TiO_3$ films grown on vicinal MgO substrates

H. Zheng, L. Salamanca-Riba,[a] and R. Ramesh[b]
Department of Materials Science and Engineering, University of Maryland, College Park, Maryland 20742

H. Li
Motorola Labs, Advanced Materials Research, Physical Sciences Research Laboratories, 7700 S. River Parkway, Tempe, Arizona 85284

(Received 13 May 2004; accepted 11 August 2004)

$Ba_{0.5}Sr_{0.5}TiO_3$ (BST) thin films were epitaxially grown on MgO vicinal substrates by pulsed-laser deposition and molecular-beam epitaxy. [001] oriented MgO substrates with 2° and 5° miscut toward [010] were selected. The nucleation of antiphase domain boundaries in the direction parallel to the step edges is greatly reduced in BST films grown on the vicinal substrates compared to the films grown on flat substrates. The reduction in antiphase domain boundaries gives rise to a higher dielectric constant when the electrodes are parallel to the direction of the steps, by about 280–460, than in the perpendicular direction. © *2004 American Institute of Physics*.
[DOI: 10.1063/1.1804609]

$(Ba_x, Sr_{1-x})TiO_3$ (BST) exhibits large dielectric constant, low dielectric dissipation factor, and low leakage current. These properties make it a promising candidate for various microelectronic and optoelectronic applications. $(Ba_x, Sr_{1-x})TiO_3$ with the composition $x=0.4$–0.6 attracts great interest since it might provide superior electric properties with a paraelectric phase at room temperature. There have been many studies on the effect of composition,[1] stress,[2–4] film/substrate interface,[5] and defects[6–8] on the dielectric properties of the BST thin films. It has been found that defects are one of the primary reasons for the degradation of the dielectric properties in BST thin films compared with the bulk value. We have recently reported that antiphase domain boundaries (ADBs) in the BST films grown on MgO substrates decrease the effective in-plane dielectric constant in the direction normal to the ADBs.[8]

There are two types of ADBs in epitaxial BST thin films grown on MgO substrates. One type corresponds to two neighboring antiphase domains having a relative shift of the lattice planes of $\frac{1}{2}[001]$ along the *c* axis (normal) to the film. The domain formation is the result of surface steps on the substrate with a height of $\frac{1}{2}a_{MgO}$ and the fact that when BST grows on MgO the TiO_2 layer always nucleates first.[9] We call this type of ADB perpendicular ADB. Another type of ADB is the "in-plane" ADB, which corresponds to adjacent domains having an in-plane lattice shift of $\frac{1}{2}[010]$ or $\frac{1}{2}[100]$ across the domain boundary. Terraces on the MgO substrate with widths equal to an integer, *n*, multiple of the MgO lattice constant a_{MgO} can induce these in-plane ADBs.[9] Another mechanism for the formation of the in-plane ADBs is solely due to the structure difference between BST (perovskite) and MgO (rocksalt).[8] Namely, on a flat (001) MgO substrate, there are two possible variants for the TiO_2 layer to nucleate. When two nuclei with different variants of the TiO_2 meet during the growth of the film an ADB forms with an in-plane phase shift of either $\mathbf{R}=\frac{1}{2}[110]$, or $\mathbf{R}=\frac{1}{2}[\bar{1}10]$. The ADBs have a shift of the lattice planes of $\frac{1}{2}[010]$ or $\frac{1}{2}[100]$ across the ADBs. Our first-principles calculations indicate that ADBs decrease the effective dielectric constant in the direction normal to the ADBs.[8] In the present study, we deposited BST films on vicinal MgO substrates in order to investigate if the formation of the ADBs could be suppressed by the preferential nucleation of TiO_2 at the step edges. We also studied the effect of ADBs on the dielectric properties of the BST films.

100-nm-thick BST ($x=0.5$) thin films were deposited on MgO [001] miscut substrates with a miscut angle of either 2° or 5° toward the [010] direction. For comparison, we also deposited BST films on a well-oriented (flat) [001] MgO substrate. The commercial miscut MgO substrates were annealed at 1100 °C for 10 min. Atomic force microscopy (AFM) operated in a vacuum environment was used to investigate the MgO surface after annealing. A KrF ($\lambda=248$ nm) excimer pulsed laser deposition (PLD) system and molecular beam epitaxy (MBE) system were used for the film deposition. During PLD growth, the substrate was held at 800 °C in a pressure of 120 mTorr O_2. A laser density of 1.2 J/cm^2 was used, corresponding to a growth rate of 5 nm/min. For the MBE growth, the alkaline earth metals (Ba/Sr) were evaporated from low-temperature effusion cells with PBN crucibles while the Ti was evaporated from a high-temperature cell with a Ta crucible. The epitaxial oxide growth was achieved using a co-deposition process in which both the alkaline earth metals and the transition element shutters were opened in a controlled oxygen environment. The fluxes were carefully calibrated to achieve the $(Ba_{0.5}Sr_{0.5})TiO_3$ stoichiometry. The growth rate for the MBE films was 1 Å/min, which was determined by measuring the period of RHEED oscillation during the oxide layer growth. Films were characterized by transmission electron microscopy (TEM) using a JEOL 4000FX operated at 300 kV. Dielectric measurements were performed using a conventional interdigital electrode consisting of 50 fingers separated by a

[a]Electronic mail: riba@umd.edu
[b]Current address: Department of Materials Science and Engineering and Department of Physics, University of California, Berkeley, CA 94720.

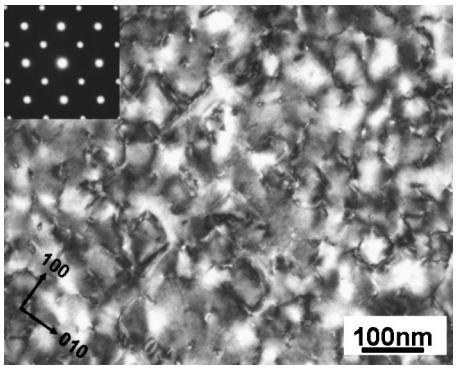

FIG. 1. Plan view TEM image of the BST thin films grown on a flat MgO substrate. The inset shows the diffraction pattern from the area.

15 μm gap. Each finger had a width of 25 μm and a length of ~0.7 cm. An HP 4192 impedance/gain analyzer was used to measure the dielectric properties. The permittivity of the BST films was extracted from the capacitance data using Gevorgian *et al.* model.[10]

Figure 1 is a plan view TEM image taken from a film grown on a flat MgO substrate. X-ray diffraction (not shown) together with electron diffraction (inset to Fig. 1) results demonstrate the high crystallinity and epitaxy of the BST films. However, a high density and randomly distributed ADBs are identified. Each domain has an average width of ~50 nm along the [100] and [010] directions, which is consistent with the results we have previously reported.[8]

In an attempt to eliminate the formation of ADBs, we grew BST films on miscut MgO surfaces. The surface of an MgO substrate with 5° miscut toward the [010] direction after annealing is shown in the AFM image in Fig. 2, which demonstrates uniform step distribution at the surface. The step height is about 0.4–0.8 nm and the terrace width is about 5–10 nm. The MgO substrate with 2° miscut toward the [010] direction after annealing has similar step height of 0.4–0.8 nm but a different terrace width of about 20–30 nm. Increasing the annealing temperature and/or annealing time

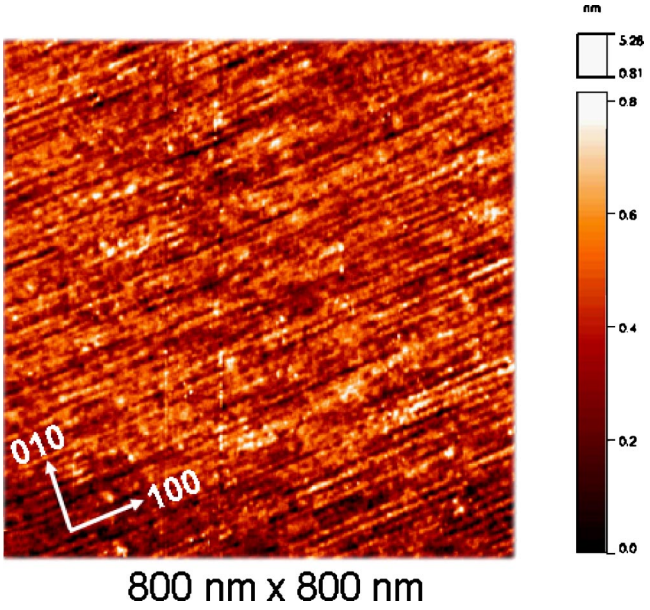

FIG. 2. (Color online) AFM image of the [001] oriented MgO substrate with 5° miscut toward [010] direction after annealing at 1100 °C for 10 min.

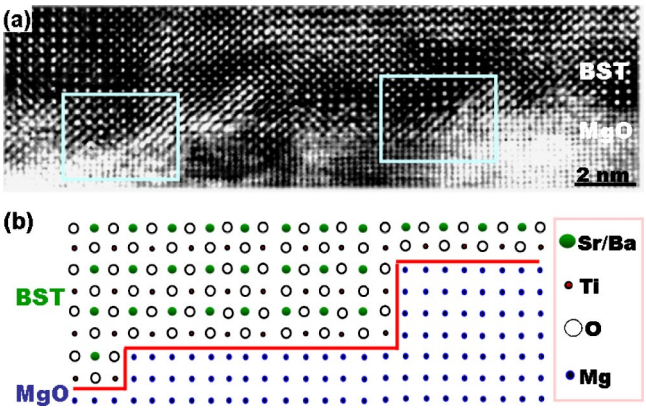

FIG. 3. (Color online) (a) Cross-section high resolution TEM image from a PLD grown BST film on an MgO substrate with 5° miscut. (b) Schematic of the atomic arrangement of a BST thin film grown on MgO with a miscut surface with step height of na_{MgO} and terrace width of $(\frac{1}{2}+n)a_{\mathrm{MgO}}$.

increases the terrace width and produces formation of step bunches.

All the films studied were epitaxial with sharp interface with the substrate. Extensive cross-section dark field and high resolution TEM studies from (010) and (100) cross-sectional samples showed that no out-of-plane ADBs formed in the BST films. Cross-section TEM samples cut along the [010] direction showed that all the steps on the MgO surface were one or two unit cells in height, see Fig. 3(a). This observation indicates that under the present annealing procedures MgO miscut substrates prefer to have steps with height equal to an integer multiple of the MgO unit cell instead of $(\frac{1}{2}+n)a_{\mathrm{MgO}}$. We also found that under these annealing conditions the terrace widths are primarily in $(\frac{1}{2}+n)$ multiples of a_{MgO}. Since TiO_2 is the first layer grown on MgO surface, the stacking of BST films can be schematically displayed as shown in Fig. 3(b). As we can see in Fig 3(b), no perpendicular ADBs are expected to form by such steps height and terrace width from the cross-section view of the film.

Plan-view dark field TEM images from the films grown on miscut substrate show that most in-plane ADBs aligned along the [100] direction. The ADBs are perpendicular to the steps on the MgO surface. And, high resolution TEM studies confirmed that these ADBs have an in-plane lattice shift of either $\frac{1}{2}[010]$ or $\frac{1}{2}[100]$, which corresponds to second type of ADBs that resulted from the symmetry difference between the film and the substrate. Figure 4(a) is a dark field image ($g=[310]$) taken from a sample grown by PLD and Fig. 4(b) is a dark field image ($g=[300]$) taken from a sample grown by MBE. Both samples were grown on MgO substrates with a 5° miscut. Both figures show that most ADBs are approximately parallel to each other with a spacing of ~50 nm and extending for ~200 nm along the [100] direction (normal to the steps). The samples grown on the substrates with 2° miscut (not shown) showed similar results.

The in-plane dielectric constant of the BST films was measured along two directions. Two sets of electrodes one parallel and one perpendicular to the substrate step edges were deposited on each sample to measure the dielectric constant along each direction. The dielectric constant obtained from the two directions indicates distinctly different values. When the electrodes were parallel to the step edges, the electric field in the films was perpendicular to the step edges. In this case, the electric field is approximately parallel to the

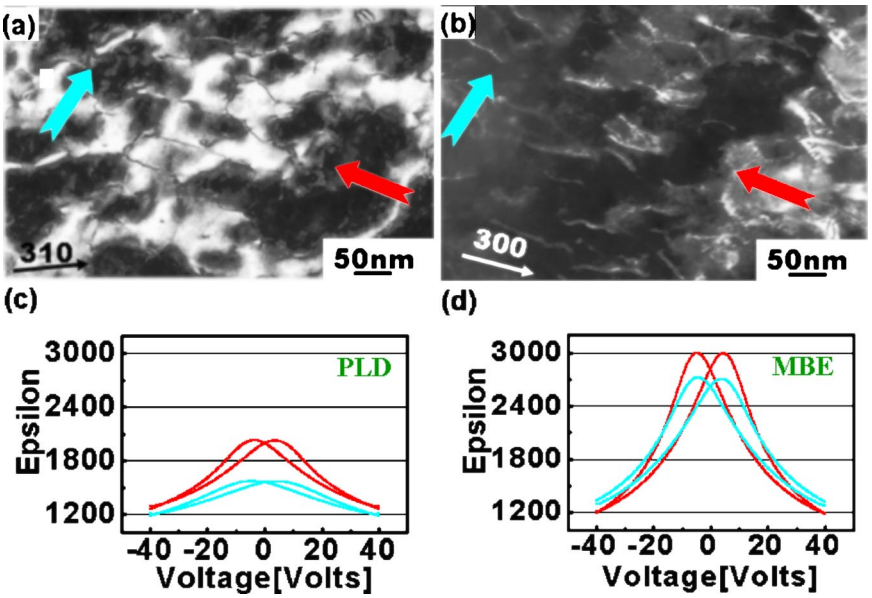

FIG. 4. (Color online) (a) Plan view $g=[310]$ dark field TEM image taken from a BST sample grown by PLD. (b) Plan view $g=[300]$ dark field TEM image taken from a BST sample grown by MBE. (c) and (d) Dielectric constant (ϵ) vs electric field (E) measured from the sample by PLD (c) and MBE (d). The two sets of curves were obtained with the electric field along the corresponding directions shown in (a) and (b), respectively.

ADBs. The dielectric constant with the electric field parallel to the ADBs ($\epsilon_{\parallel}$) is much higher than that obtained when the electric field is perpendicular to the ADBs ($\epsilon_{\perp}$) [see Figs. 4(c) and 4(d)]. In the PLD sample, $\Delta\epsilon=\epsilon_{\parallel}-\epsilon_{\perp}\sim 460$, which is about a 30% difference in the dielectric constant along the two directions. In the MBE sample, $\Delta\epsilon$ is ~ 280, which corresponds to $\sim 10\%$ difference in the dielectric constant in the two directions. These results are consistent with our previous first-principles calculations that show that ADBs decrease the effective dielectric constant in the direction normal to the ADBs.[8] The static dielectric tensor can be expressed as

$$\epsilon_{\alpha\beta}=\epsilon_{\alpha\beta}^{\infty}+\frac{4\pi}{\Omega}\sum_{\lambda}S_{\lambda,\alpha\beta}/\omega_{\lambda}^{2},$$

where $\epsilon_{\alpha\beta}^{\infty}$ is the dielectric constant at high frequency, Ω is the unit cell volume, $S_{\lambda,\alpha\beta}=[\Sigma_{\kappa,\gamma}Z_{\kappa,\alpha\gamma}^{*}U_{\lambda}(\kappa,\gamma)]\times[\Sigma_{\kappa',\delta}Z_{\kappa',\beta\delta}^{*}U_{\lambda}(\kappa',\delta)]$ is the mode oscillator strength tensor $Z_{\kappa,\alpha\gamma}^{*}$ is the effective Born charge tensor for each atom, $U_{\lambda}(\kappa,\gamma)$ are the eigendisplacements of the force constant matrix, and ω_{λ} are the infrared-active phonon frequencies. The calculated dielectric response perpendicular to the ADBs is greatly reduced compared with the ideal $SrTiO_3$. This reduction is directly attributed to the breaking of infinite Ti–O chains normal to the ADBs. The dielectric constant from the sample grown by MBE shows a much higher value of $\epsilon_{\parallel}\sim 3000$ compared with $\epsilon_{\parallel}\sim 2020$ for the PLD sample. This is probably because the films grown by MBE are of higher quality than the PLD films.

We propose the following mechanism for the growth of BST on the miscut MgO substrates. When BST films first nucleate, the nuclei prefer to form at step edges in order to lower the surface energy. Then, the growth of the film flows from the step edge along the surface of the terrace. Since the widths of the terraces are in $(\frac{1}{2}+n)$ multiples of a_{MgO} and much smaller than the ~ 50 nm average width of the ADBs observed in films grown on flat substrates, it is less likely for ADBs to form parallel to the step edges of the MgO surface. However, antiphase domains can still form from the nucleation of equivalent domains along the terrace. The latter nucleation induces ADBs perpendicular to the step edges.

In summary, the BST thin films grown on [001] oriented MgO substrates with 2° and 5° miscut toward [010] can considerably decrease the density of ADBs in the direction parallel to the step edges. This reduction results from the preferential nucleation of domains at step edges. The dielectric constant was much higher in the direction parallel to the step edges than in the perpendicular direction.

This work was supported by the NSF-MRSEC under Contract No. DMR-00-80008. The NSF-MRSEC has provided support for the Pulsed Laser Deposition System used in this research.

[1] Y. Gim, T. Hudson, Y. Fan, C. Kwon, A. T. Findikoglu, B. J. Gibbons, B. H. Park, and Q. X. Jia, Appl. Phys. Lett. **77**, 1200 (2000).
[2] J. S. Horwitz, W. Chang, W. Kim, S. B. Qadri, J. M. Pond, S. W. Kirchoefer, and D. B. Chrisey, J. Electroceram. **4**, 357 (2000).
[3] H. Li, A. L. Roytburd, S. P. Alpay, T. D. Tran, L. Salamanca-Riba, and R. Ramesh, Appl. Phys. Lett. **78**, 2354 (2001).
[4] Y. I. Yuzyuk, P. Simon, I. N. Zakharchenko, V. A. Alyoshin, and E. V. Sviridov, Phys. Rev. B **66**, 052103 (2002).
[5] H.-J. Gao, C. L. Chen, B. Rafferty, S. J. Pennycook, G. P. Luo, and C. W. Chu, Appl. Phys. Lett. **75**, 2542 (1999).
[6] C. L Canedy, H. Li, S. P. Alpay, L. Salamanca-Riba, A. L. Roytburd, and R. Ramesh, Appl. Phys. Lett. **77**, 1695 (2000).
[7] W. J. Kim, W. Chang, S. B. Qadri, J. M. Pond, S. W. Kirchoefer, D. B. Chrisey, and J. S. Horwitz, Appl. Phys. Lett. **76**, 1185 (2000).
[8] H. Li, H. Zheng, L. Salamanca-Riba, R. Ramesh, I. Naumov, and K. Rabe, Appl. Phys. Lett. **81**, 4398 (2002).
[9] J. C. Jiang, Y. Lin, C. L. Chien, C. W. Chu, and E. I. Meletis, J. Appl. Phys. **91**, 3188 (2002).
[10] S. S. Gevorgian, T. Martinsson, P. L. J. Linner, and E. L. Kollberg, IEEE Trans. Microwave Theory Tech. **44**, 896 (1996).